

# Determining water saturation in low resistivity - low contrast formations using the Leverett J-Function: A case study of well X, field Y, Cuu Long basin

NGUYEN Viet An<sup>1,3</sup>, TRUONG Quoc Thanh<sup>1,3</sup>, TRAN Van Xuan<sup>1,3</sup>, NGUYEN Tuan<sup>2,3</sup>,  
DANG Truong An<sup>2,3</sup>, MAI Huu Xuan<sup>1,3</sup>, NGUYEN Huynh Thong<sup>1,3</sup>, LUONG Bao Minh<sup>1,3</sup>,  
NGUYEN Xuan Kha<sup>1,3\*</sup>

<sup>1</sup> University of Technology, Ho Chi Minh City, Vietnam

<sup>2</sup> University of Science, Ho Chi Minh City, Vietnam

<sup>3</sup> Vietnam National University, Ho Chi Minh City, Vietnam

\* Corresponding email: [nxkha@hcmut.edu.vn](mailto:nxkha@hcmut.edu.vn)

**Abstract:** The Field Y, located in the Cuu Long Basin, Vietnam, is currently being explored and developed for its potential in the Lower Miocene reservoirs. However, one of the key challenges faced by geologists and well log analysts is the presence of low-resistivity, low-contrast (LRLC) pay zones, which hinder the accuracy of log interpretation and evaluation. Calculating water saturation in these low-resistivity zones using conventional interpretation techniques often results in significant errors, potentially leading to the misidentification of productive intervals. This paper determines the primary causes of low resistivity, including the influence of invasion zones, well and formation dip, limitations of logging tools, grain size, clay content and distribution, and formation water salinity. The authors propose the Leverett (J-function) method, independent of resistivity, to calculate water saturation. This method aims to improve the calculation of net pay thickness in the Well X, Field Y. Results show that in the Lower Miocene formation, the net pay thickness of the BI.2.20 interval increased by 2,773 meters and the BI.1.20 interval increased by 1,981 meters. This improvement helps to avoid misidentification of productive zones and ultimately increase recoverable reserves.

**Keywords:** Cuu Long Basin; Low resistivity – low contrast; Lower Miocene; Leverett J-function; well logging

## 1. Introduction

The study area, Field Y, is located in the northwestern part of the Cuu Long Basin, offshore southeastern Vietnam. It is situated approximately 70 m below sea level, 160 kilometers east of Vung Tau, 20 km east of STV Field, and 35 km northeast of RD Field. The primary production targets in the Well X, Field Y, are the laminated shaly sand formation within the BI.2.20 unit of the Bach Ho Formation, with a secondary target being the sand intervals within the BI.1.20 unit, in the Lower Miocene [1].

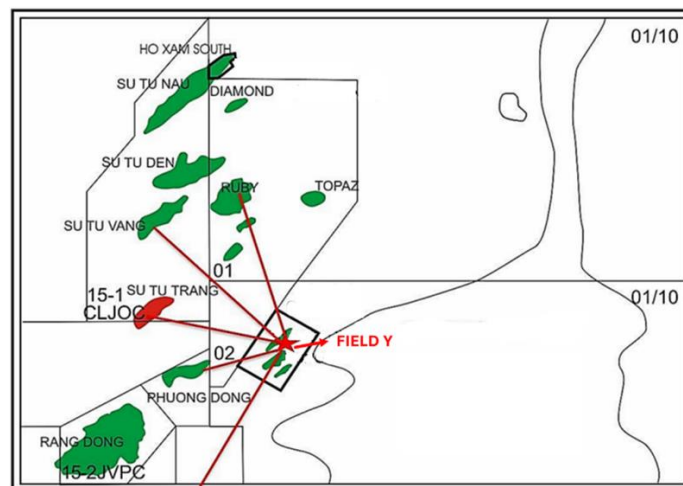


**Fig. 1.** Sketch of location of Field Y, Cuu Long Basin, Vietnam

Within the Lower Miocene Formation, Cuu Long Basin, low-resistivity, low-contrast pay zones are a common feature. In these zones, the deep resistivity measurements typically range from 1 – 5 Ohmm [2, 4, 6, 8]. The causes of this low resistivity can include drilling technology factors, limitations of logging

equipment, as well as the specific geological characteristics of the study area. Well X is the fifth production well of the drilling 8-production well campaign in the Field Y (Fig. 1) and the production well for the Lower Miocene.

## 2. Causes of low resistivity – low contrast pay

### \* Invasion zone effects:

Drilling in the Field Y typically employs water-based drilling mud, which is electrically conductive. To prevent borehole instability (caving and swelling) during drilling and well logging operations, mud pressure is maintained above formation pressure. This pressure differential can cause the drilling mud to penetrate deep into the formation, creating invasion zones around the wellbore. These invasion zones are categorized into three distinct groups: the fully invaded zone, the transition zone, and the uninvaded zone [3]. The Field Y reservoir rocks exhibit high porosity (15 - 20%) and permeability (50-300 mD), leading to extensive invasion zones extending further than the investigation depth of most resistivity logging tools. Consequently, measured resistivity values are often lower than the true formation resistivity.

### \* Formation dip and well deviation:

Deep wells are rarely drilled perfectly perpendicular to the formation; rather, they typically deviate at an angle. When the angle between the wellbore and the formation deviates from 90 degrees, it leads to errors in resistivity measurements because the logging tools are sensitive to the well's inclination. The smaller the angle between the wellbore and the formation, the greater the distortion in resistivity readings. Therefore, correcting for inclination is essential during data processing and interpretation to eliminate errors in resistivity and other related measurements[3]. Trajectory of the Well X in the Field Y is presented in Fig. 2. Measured depth (MD) is the actual depth measured from the surface to a point along a wellbore. True vertical depth subsea (TVDSS) is the vertical depth from the surface to the same point, calculated to account for the angle of inclination of the strata.

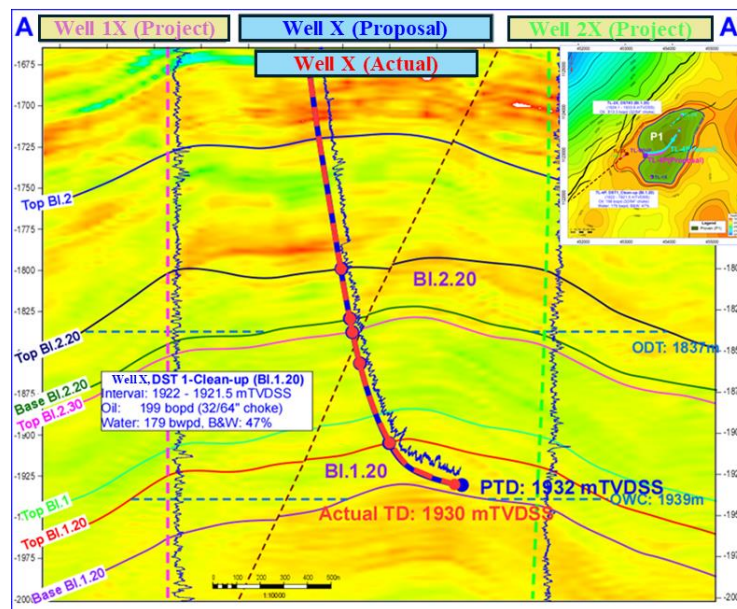


Fig. 2. Actual well path of Well X [1]

### \* Limitations in logging tool investigation depth:

The investigation depth of logging tools varies depending on the tool type and the intended application. In the Field Y, the high porosity and permeability of the reservoir lead to extensive invasion zones, where drilling mud penetrates the formation. If water-based mud is used, as in the wells of this field, resistivity measurements into formation will often underestimate the true formation resistivity. Therefore, if the investigation depth of the logging tool is shallower than the radius of mud invasion, this can contribute to the observed low resistivity readings, even in thinly-bedded formations. [3, 5, 9].

### \* Influence of grain size:

Sedimentary rocks are formed from the accumulation and cementation of sediment particles derived from the weathering and erosion of pre-existing rocks. Based on particle size, these sediments are classified as: gravels (particles larger than 1 mm), sandstones (particles between 1-0.1 mm), siltstones (particles between 0.1-0.01 mm), and shales (particles smaller than 0.01 mm). These sedimentary particles form the

framework of the rock. As particle size decreases, the specific surface area of the rock increases, leading to a higher amount of bound water and increased cation exchange capacity. This results in sandstones with a high content of dispersed clay or shales, where finer grains hold a greater volume of bound water, consequently lowering measured resistivity [3, 4, 7, 8]. The grain size of clay and siltstone accounts for a significant portion, which has lowered the resistivity value (Table 1).

**Tab. 1.** Grain size of rock material in Well X

No.		1	2	3	4	5	6	7	8	9
Sample Depth		2070-2075	2125-2130	2165-2170	2240-2245	2300-2305	2325-2320	2365-2370	2405-2410	2560-2565
Phi Scale (%)	Millimetre scale (mm)	Volume (%)	Volume (%)	Volume (%)	Volume (%)	Volume (%)	Volume (%)	Volume (%)	Volume (%)	Volume (%)
< -2.0	> 4	2.0				1.0	1.0			
-1.5 - -2.0	2.83 - 4	3.0	2.0	1.0	4.0	4.0	4.0	1.0	2.0	
-1 - -1.5	2 - 2.83	6.0	2.0	4.0	4.0	3.0	6.0	2.0	3.0	
-0.5 - -1.0	1.41 - 2	9.0	3.0	5.0	9.0	4.0	4.0	3.0	5.0	
0.0 - -0.5	1 - 1.41	7.0	2.0	2.0	8.0	5.0	5.0	4.0	4.0	
0.5 - 1.0	0.71 - 1	5.0	2.0	3.0	7.0	10.0	10.0	8.0	7.0	1.0
1.0 - 0.5	0.5 - 0.71	3.0	8.0	9.0	15.0	18.0	17.0	14.0	15.0	4.0
1.5 - 1.0	0.35 - 0.5	8.0	16.0	25.0	19.0	10.0	10.0	18.0	14.0	6.0
1.0 - 1.5	0.25 - 0.35	5.0	20.0	15.0	7.0	9.0	8.0	14.0	13.0	10.0
1.5 - 2.0	0.175 - 0.25	12.0	10.0	9.0	12.0	7.0	9.0	9.0	12.0	42.0
2.0 - 2.5	0.125 - 0.175	17.0	8.0	10.0	5.0	11.0	9.0	6.0	12.0	27.0
2.5 - 3.0	0.088 - 0.125	13.0	10.0	6.0	6.0	9.0	10.0	14.0	9.0	10.0
3.0 - 3.5	0.063 - 0.088	4.0	9.0	7.0	1.0	5.0	5.0	4.0	3.0	
3.5 - 4.0	0.044 - 0.063	6.0	8.0	4.0	3.0	4.0	2.0	3.0	1.0	
4.0 - 4.5	0.031 - 0.044									
> 5.0	< 0.031									
		100.0	100.0	100.0	100.0	100.0	100.0	100.0	100.0	100.0

**\* Clay distribution:**

Clay minerals can be distributed within reservoir rocks in three primary forms: laminated shales, dispersed clays, and structural clays [9]. When dealing with laminated shaly-sand sequences or thinly bedded formations, traditional resistivity logging methods tend to measure an average resistivity across the sand, silt, and clay layers [9, 10]. This averaging process can negatively impact the accuracy of water saturation calculations [8]. During log interpretation for the Well X, identifying laminated shaly-sand intervals can be achieved effectively by examining the Gamma Ray log and Gas Index. The Gamma Ray log is a valuable tool for distinguishing sand from shale due to its ability to measure the natural radioactivity of the rock. Thin beds are characterized as having a thickness of 0.1 – 1 m. Typically, thin beds are thinner than the vertical resolution of conventional logging tools [3, 10, 11]. Through the well logging interpretation, the total thickness of the BI.2.20 reservoir is about 71 m, divided into 16 zones with potential to contain hydrocarbons (Fig. 3). These zones satisfy the cut off values of shale volume, porosity and water saturation mentioned in Table 4. Most sand zones are less than 1 m thick, classifying them as thin beds.

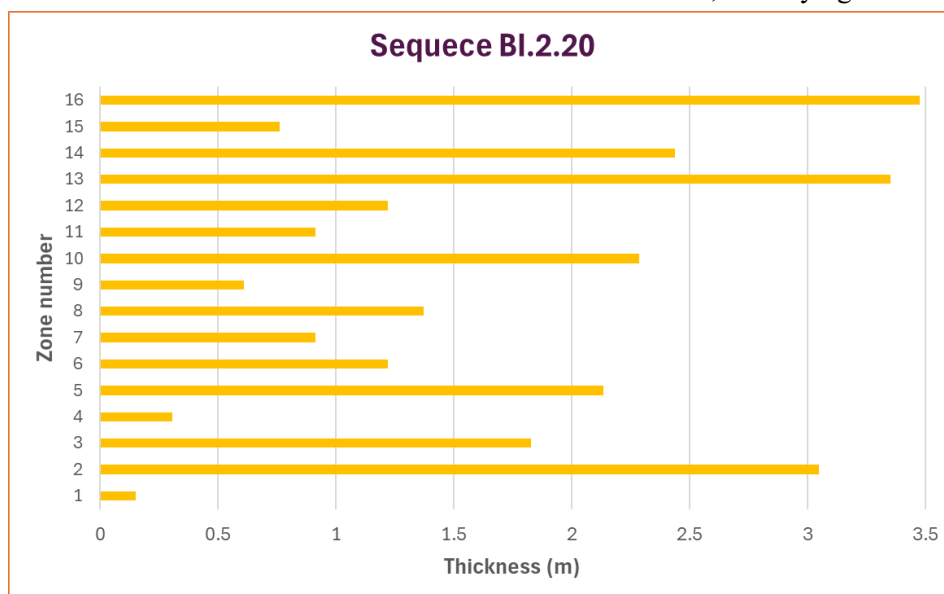


**Fig. 3.** Thickness of the potential zones within the Sequence BI.2.20

The Gas Index also plays a crucial role in identifying laminated shaly-sand intervals. On the Gas Index log, sand layers containing gas are often marked by a sharp increase in gas index compared to shale layers or zones with no gas presence. In Figure 4, Gas Data column shows significant fluctuations which also contributes to proving the presences of thin-bed layers.

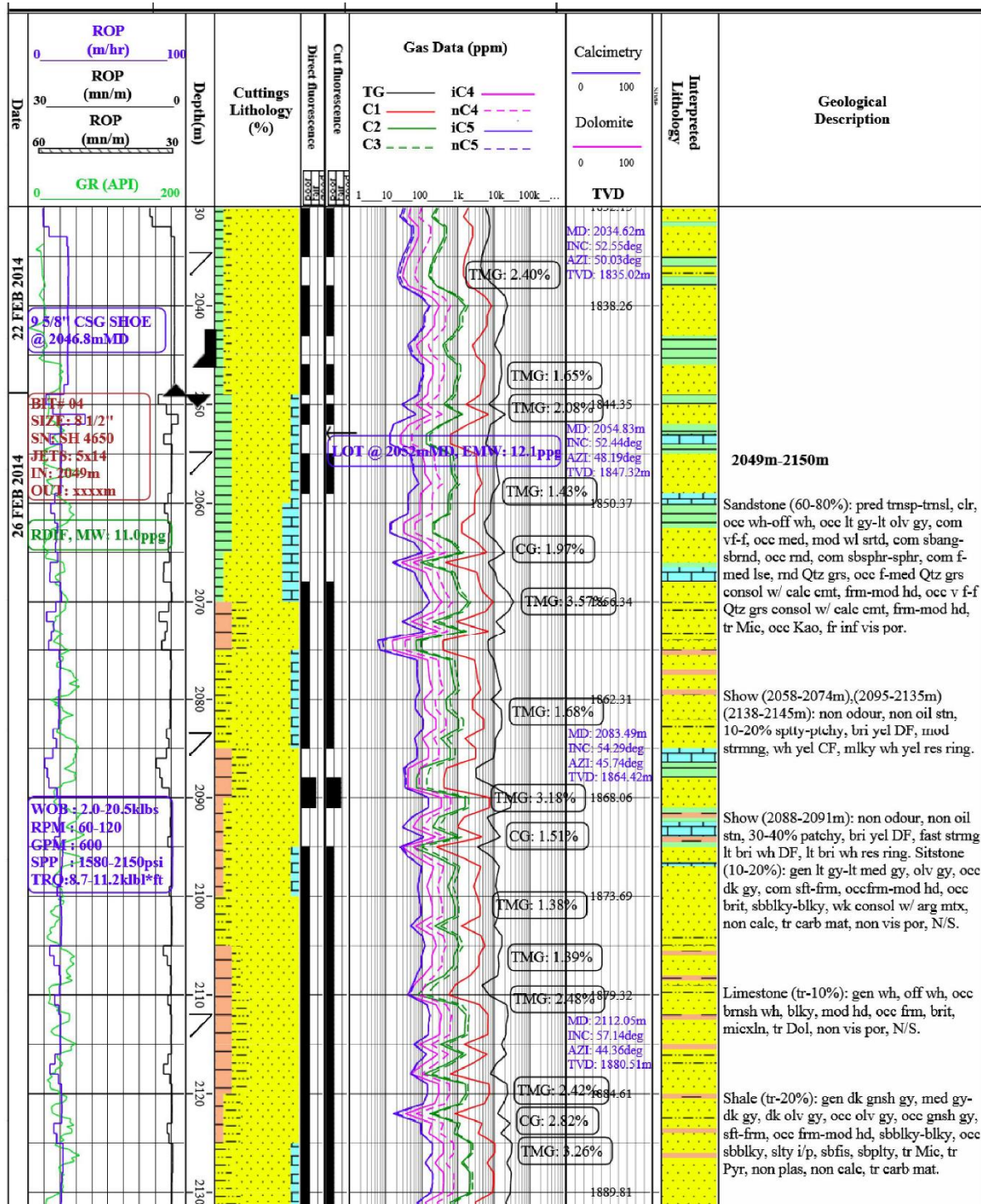


Fig. 4. Masterlog of sequence BI.2.20 (with TG: Trip gas, TMG: Formation gas, AZI: Azimuth, INC: Inclination)

**\* Formation water salinity:**

Higher formation water salinity results in lower formation water resistivity, and vice versa. When comparing two reservoirs with similar porosity and saturation, the reservoir with higher salinity will exhibit lower resistivity [8, 12]. In the Field Y, the Lower Miocene reservoir within the Bach Ho Formation exhibits formation water salinity ranging from 34,000 ppm to 38,700 ppm. The Upper and Lower Con Son formations of the Middle Miocene age also show similar salinity levels. This indicates a general trend of increasing salinity from the Oligocene to the Miocene, corresponding to a gradual marine transgression

during this period. The presence of the thick Rotalia shale layer at the top of the Miocene marks the peak of this transgression, consistent with the overall geological history of the Cuu Long Basin.

**\* Bound water and Cation Exchange Capacity (CEC):**

Water that surrounds the mineral grains of sand and clay minerals is known as bound water or pore-lining water. This type of water cannot be extracted during primary or secondary recovery operations. Clay minerals typically exhibit a high surface area and contain a significant amount of cations (Table 2). The higher the cation exchange capacity (CEC) of the clay, the lower the measured resistivity of the rock [2, 12]. This is because clay minerals have a negatively charged surface, attracting cations such as Na<sup>+</sup> and K<sup>+</sup> when they are dry. When submerged in water, these cations are released, increasing the water's conductivity [8, 13]. CEC is measured in milliequivalents per 100 grams of dry clay and quantifies the clay's ability to release cations. Clays with a high CEC have a greater impact on lowering resistivity than clays with a low CEC. For example, montmorillonite, also known as smectite, has a CEC of 80 to 150 meq/100 g, while kaolinite's CEC is only 3 to 15 meq/100 g [4].

**Tab. 2.** Cation Exchange Capacity (CEC) of clay minerals

Clay minerals	Specific surface area (m <sup>2</sup> /g)	CEC (meq/g)
<b>Kaolinite</b>	12 – 45	0.02 – 0.15
<b>Chlorite</b>	25 – 130	0.03 – 0.42
<b>Illite</b>	90 – 120	0.1 – 0.4
<b>Montmorillonite (Smectite)</b>	500 – 1000	0.8 – 1.7

The amount of bound water is also proportional to the thickness of the bound water layer surrounding the clay particles. Montmorillonite is known for its high activity, large surface area, and thick hydration layer within its crystal lattice, which allows it to retain more water than other clay minerals [6]. Consequently, reservoirs with a high content of montmorillonite will exhibit higher calculated water saturations and lower measured resistivity than expected.

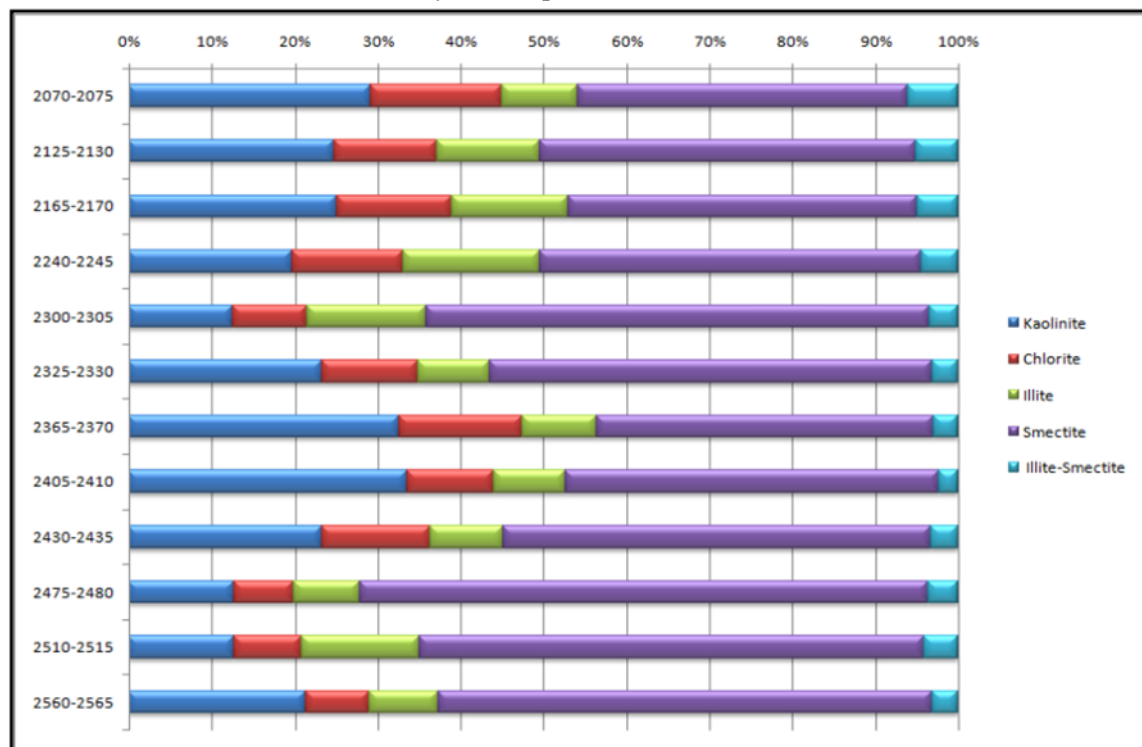


**Fig. 5.** Summary of XRD data for clay fraction in depth intervals 2070 – 2075 m (BI.2.20) and 2325 – 2435 m (BI.2.20) in Well X

Montmorillonite content exceeds 50% (Fig. 5), which is a major factor contributing to the low resistivity of the reservoir rock and negatively impacts its porosity and permeability.

### 3. Methodology

#### 3.1 Water saturation calculation from traditional method

##### \* Input data

Based on the core data of the Lower Miocene, parameters including a, m, n and cut-off values are determined as in Table 3:

**Tab. 3.** Input parameters

Field	Formation	Rw @ 25°C (Ohmm)	Formation water salinity, ppm	a	m	n	Cut-off values (%)		
							Vsh	NPHI	Sw
Y	Lower Miocene	0.18	34000	1	1.74	1.83	40	10	70

##### \* Shale volume, Porosity and Water saturation calculation

Shale volume (Vsh) is calculated using the Gamma Ray and Neutron-Density logs, with the Clavier equation employed to adjust the shale volume calculated using the linear method. Porosity is determined through the combined Neutron-Density method, utilizing a formula that integrates values from both methods. Water saturation is calculated using the Modified Simandoux model, an extension of the Simandoux equation from 1963, to account for the increased conductivity of the reservoir rock due to dispersed clay content.

#### 3.2 Water saturation calculation from Leverett (J-Function) method

The Leverett method, describing the relationship between capillary pressure and water saturation, was developed by Leverett in 1941. The J-function (1), built upon the Leverett method, provides a resistivity-independent approach to calculate water saturation, particularly valuable in evaluating low-resistivity reservoirs as Field Y [3, 14, 15].

$$J(S_w) = \frac{P_c}{\sigma \cos\theta} \sqrt{\frac{k}{\phi}} \quad (1)$$

P<sub>c</sub>: Capillary pressure (psia),

σ: Interfacial tension (dyn/cm),

θ: Contact angle (degree),

k: Permeability (mD),

Φ: Porosity.

This method improves the accuracy and efficiency of water saturation estimation in complex geological settings. To develop the Leverett J-function, core data from the well X were analyzed to determine relevant parameters (2).

$$P_{C(res)} = P_{C(lab)} \frac{(\sigma \cos\theta)_{res}}{(\sigma \cos\theta)_{lab}} \quad (2)$$

P<sub>c(res)</sub>: Capillary pressure (psia) in reservoir,

P<sub>c(lab)</sub>: Capillary pressure (psia) in laboratory,

σ<sub>c(res)</sub>: Interfacial tension (dyn/cm) in reservoir (= 30 dyn/cm),

σ<sub>c(lab)</sub>: Interfacial tension (dyn/cm) in laboratory (= 72 dyn/cm),

θ<sub>res</sub>: Contact angle (degree) in reservoir (= 30°),

θ<sub>lab</sub>: Contact angle (degree) in laboratory (= 0°).

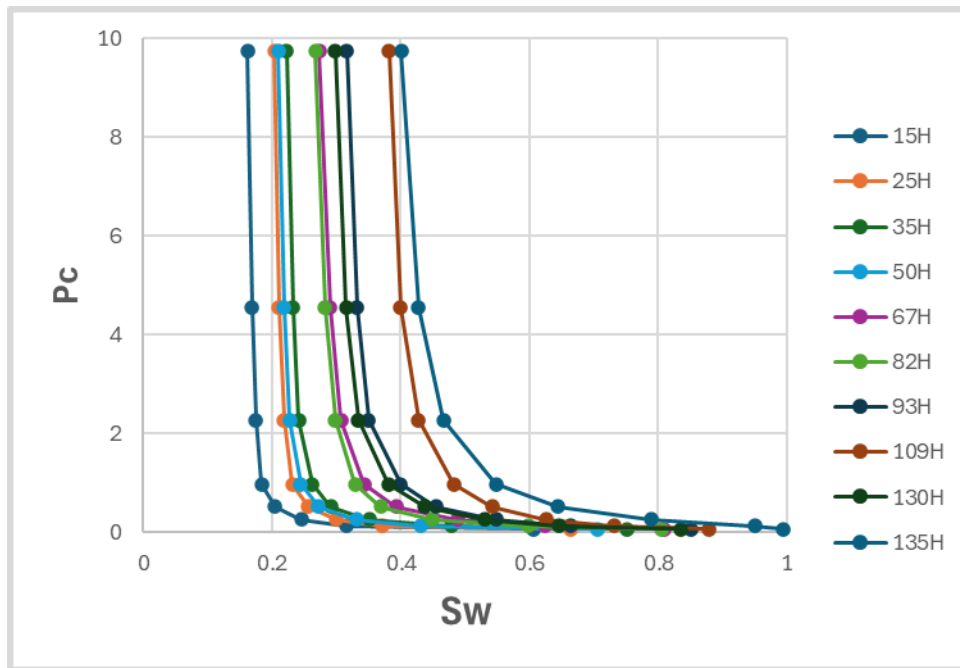


**Fig. 6.** Relationship between Sw vs. Pc according to the core data

According to the Leverett method, the relationship between  $J(Sw)$  and Sw was established based on the input data, which are obtained from laboratory experiment between Pc and Sw. There are 10 cores, 15H – 135H, (Fig. 6) whose Sw were measured at different Pc values (0, 1, 2, 4, 8, 15, 35, 70, 150 psig).

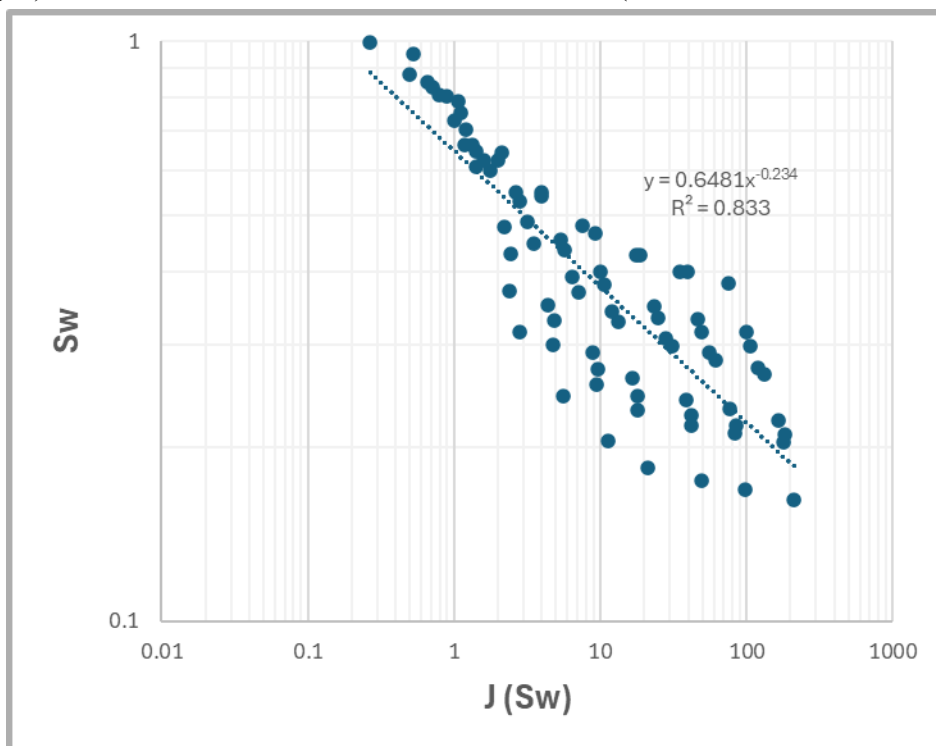


**Fig. 7.** Relationship between Leverett J-Function,  $J(Sw)$  and water saturation, Sw according to core data

Therefore,  $Sw = 0.6481(J)^{-0.234}$  (Fig. 7), this relationship is used to calculate Sw for intervals where core data is not available, and the results are compared with Sw calculated from resistivity using conventional method.

#### 4. Results and discussion

##### \* From the traditional method

The Well X was drilled to a total depth of 2607 m MD (1930 m TVDSS), penetrating formations from the youngest to oldest: the Bien Dong, Dong Nai, Upper and Lower Con Son, and Upper and Lower Bach Ho formations (BI.2.20 and BI.1.20 reservoirs). The study in Well X focuses solely on the Lower Miocene

reservoir, specifically the Upper and Lower Bach Ho formations. This interval extends from 1939 m MD (1729 m TVDSS) to 2607 m MD (1930 m TVDSS).

According to the reservoir classification report, the BI.2.20 and BI.1.20 intervals in the Well X have been classified as P1 reserves classification and currently exhibit stable hydrocarbon production. P1 reserves classification refers to a category of hydrocarbon reserves in Vietnam's classification system, signifying reserves that are considered proven and economically recoverable with high confidence. These are the two main intervals used for hydrocarbon reserve calculations in the Well X.

The BI.2.20 interval has a significant net pay thickness exceeding 26 meters, with an average porosity of approximately 14.1% and an average water saturation of about 56%.

The BI.1.20 interval exhibits the greatest net pay thickness within the Lower Miocene section of the Well X, reaching a total of 65 meters for the entire interval (which is nearly 117 meters thick). The average shale volume is relatively low at 4.5%, the average porosity is around 18.7%, and the water saturation is similar to the Upper Bach Ho intervals, around 56.8%.

The detailed results of the well log interpretation are summarized in Table 4:

**Tab. 4.** Results of traditional method of Sw determination

Sequences	Top (mMD)	Bottom (mMD)	Gross	Net reservoir	Net pay	Av VSH	Av PHIE	Av SW
BI.2.20	2049.5	2120	70.5	31.333	26.031	19.6	14.1	56
BI.1.20	2317	2434	117	78.486	65.227	4.5	18.7	56.8

**\* From Leverett (J-Function) method**

Currently, the oil-water contact (OWC) of the BI.1.20 interval is located at 1939 m TVDSS. This interval is considered to have a significant net pay thickness, exceeding 65 meters, as determined by both conventional and the Leverett (J-function) methods. The calculated water saturation values (Sw) using both conventional and Leverett (J-function) methods show a strong correlation (Fig. 8). The Leverett J-function has been validated as a suitable method for calculating Sw in typical BI interval, particularly those with a considerable net pay thickness.

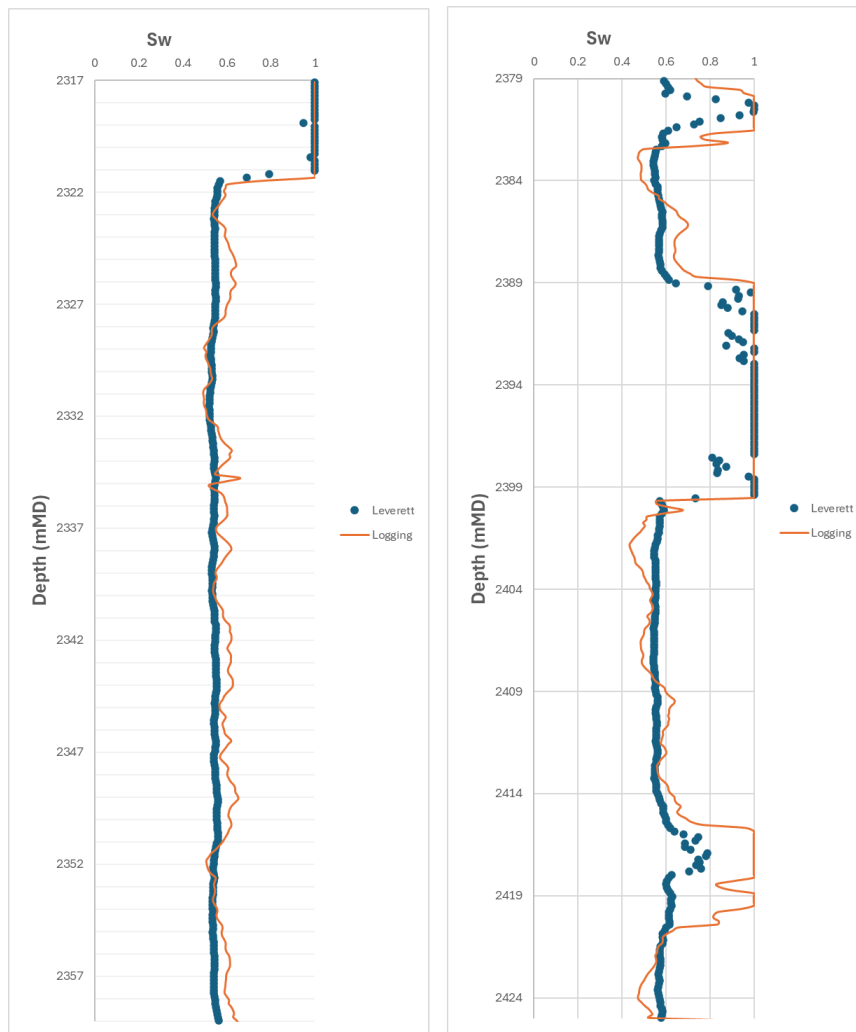


**Fig. 8.** Comparison of water saturation from the Leverett J-Function method and the traditional method (resistivity logging) in the BI.1.20 interval

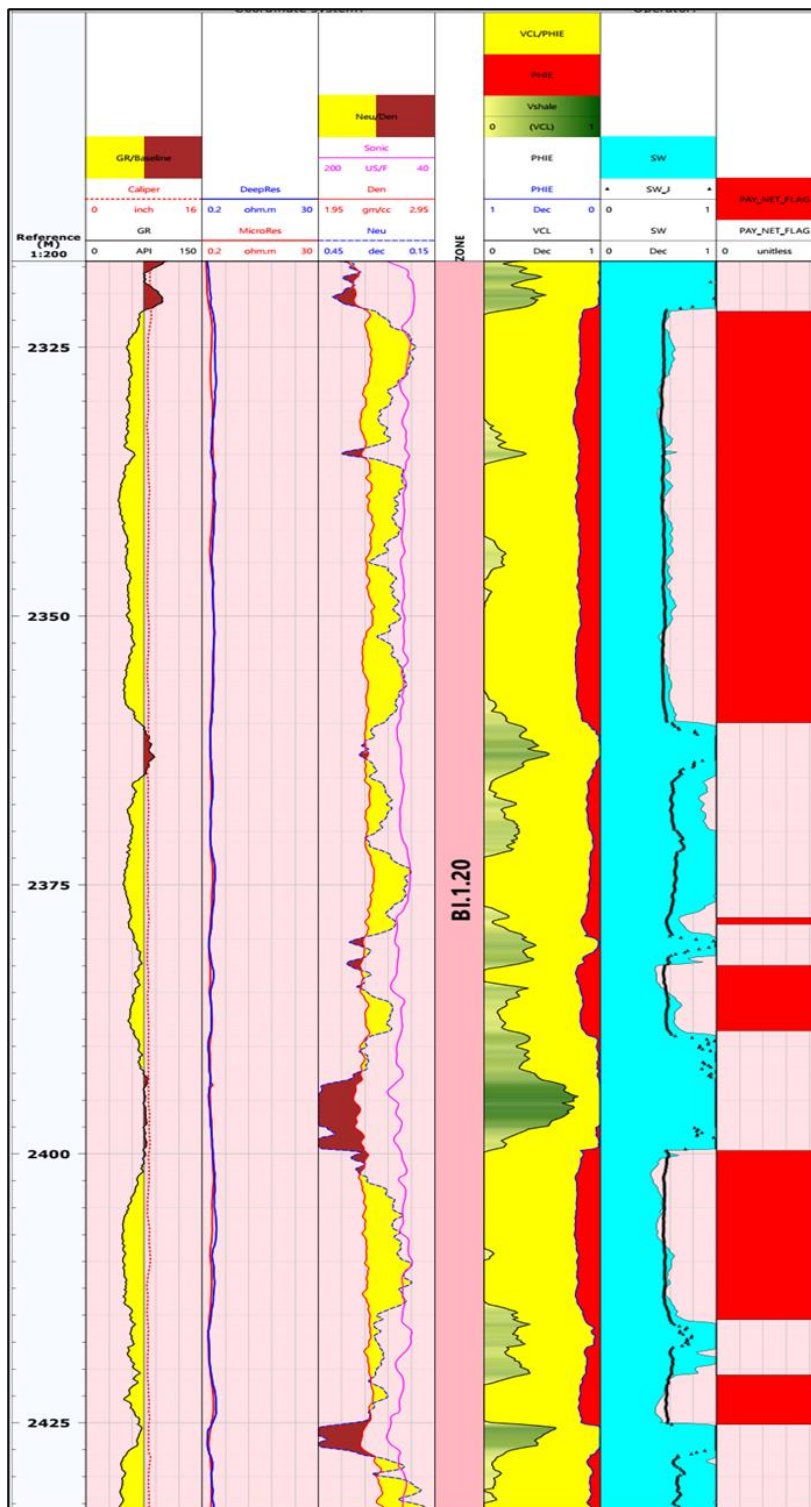


**Fig. 9.** Well logging interpretation of BI.1.20 by Techlog software

The well logging interpretation was performed with TECHLOG 2015.3 (Montpellier, South of France) software (Figs 9 and 11). At the moment, Techlog software is a commercial product developed and maintained by Schlumberger. This software provides comprehensive visualization and analysis tools for well log data, enabling interpretation of geological formations and reservoir characteristics. It facilitates the correlation and integration of various geophysical logs, aiding in the understanding of subsurface structures and fluid saturations.

The Leverett J-function was also applied to calculate the water saturation for the BI.2.20 interval. The current oil-water contact (OWC) for this interval is at 1845 m TVDSS, corresponding to the highest oil column height at a depth of 1797.147 m TVDSS. The results of the water saturation for the BI.2.20 interval in Well X are presented as in Fig. 10:

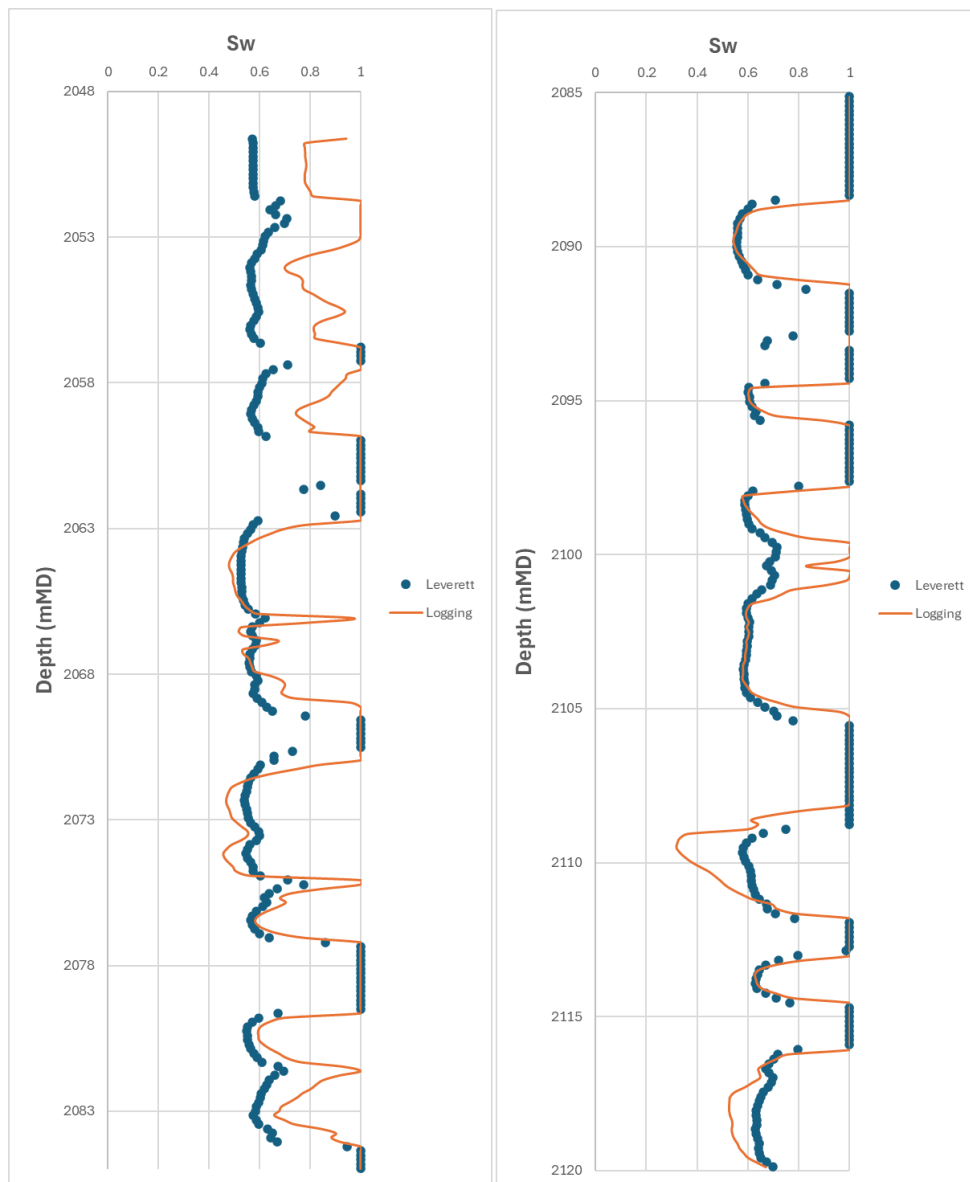


**Fig. 10.** Comparison of water saturation from the Leverett J-Function method and the traditional method (resistivity logging) in the BI.2.20 interval

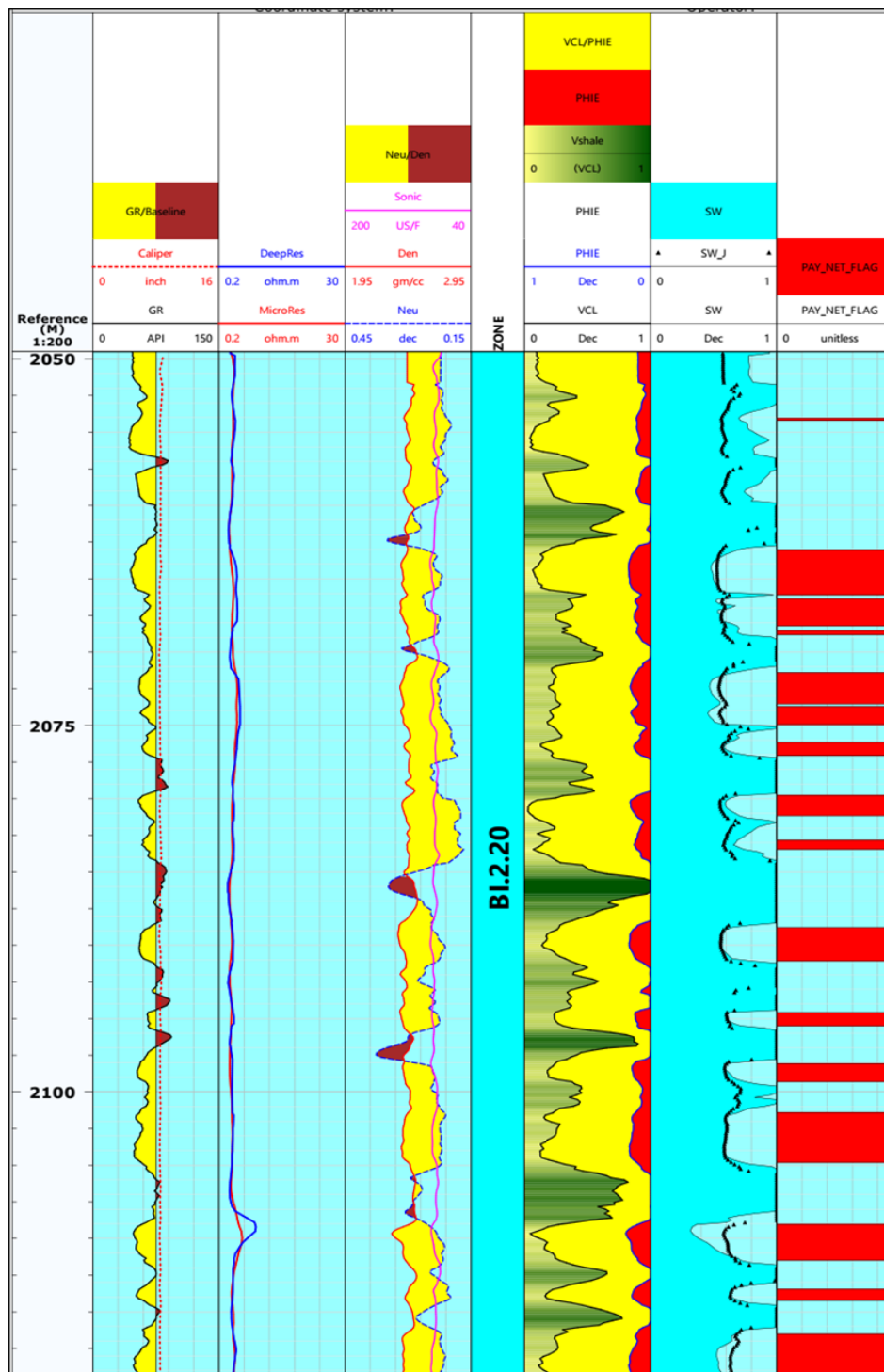


**Fig. 11.** Well logging interpretation of BI.2.20 by Techlog Software

Based on the analysis of petrographic, geological, well log, composite log, and master log data, the BI.2.20 interval is characterized as a thin-bedded, laminated shaly-sand reservoir. Furthermore, DST, MDT, and mud log data confirm the presence of hydrocarbons in this zone. However, the resistivity readings in this interval exhibit relatively low values, ranging in 2 - 5 Ohmm, indicating a low-resistivity pay zone.

**\* Comparison of water saturation calculation methods: Leverett J-Function and traditional methods**

The results demonstrate that Sw calculated using the Leverett J-function is generally consistent with Sw derived from resistivity measurements (Table 5). However, the Leverett J-function method consistently yields lower Sw values compared to the traditional approach. This finding suggests that calculating Sw independently from resistivity measurements provides a promising alternative for evaluating reservoir potential and improving the estimated net pay thickness of hydrocarbon-bearing intervals. Notably, this method is particularly applicable for thin-bedded formations and those exhibiting low resistivity due to factors previously discussed.

**Tab. 5.** Result of comparison of Sw from traditional method and Leverett J-Function method

Sequences	Top (mMD)	Bottom (mMD)	Gross	Net reservoir	Net pay (m) - Traditional method	Net pay (m) - J Function	Av VSH	Av PHIE	Av SW - Traditional method	Av SW - J Function
BI.2.20	2049.5	2120	70.5	31.333	26.031	<b>28.804</b>	19.6	14.1	56	<b>58.2</b>
BI.1.20	2317	2434	117	78.486	65.227	<b>67.208</b>	4.5	18.7	56.8	<b>55.1</b>

The results indicate that the J-function method has significantly improved the net pay thickness of the BI.2.20 interval by 2,773 m and the BI.1.20 interval by 1,981 m compared to the traditional resistivity-dependent calculation method.

## 5. Conclusion

Based on a comprehensive analysis of petrographic data, mudlogs, well logs, and DST (Drill Stem Test) results, this study has drawn the following conclusions: In the Lower Miocene formation of the Field Y, Cuu Long Basin, the Well X currently targets and produces from two intervals: BI.2.20 and BI.1.20. The BI.1.20 interval is currently producing hydrocarbons with a significant net pay thickness. The BI.2.20 interval, exhibiting a resistivity ranging in 2 - 5 Ohmm, is a low-resistivity pay zone. The direct causes of this low resistivity include: extensive invasion zone effects; formation dip and well deviation, logging tool depth limitations, grain size effects, clay distribution within the reservoir rock, notably thin-bedded, interbedded sand-silt-shale layers, high formation water salinity, and high bound water content due to the large specific surface area of the grains. Illite and smectite clay minerals constitute a significant proportion (over 50%) of the clay content, exceeding other clay minerals like chlorite and kaolinite.

The Leverett J-function method for calculating water saturation yielded an average value of approximately 58.2% for the BI.2.20 interval and 55.1% for the BI.1.20 interval, closely aligning with the basic well log interpretation model. Notably, after applying the cutoff values for results from the Leverett J-function method, the net pay thickness of the BI.2.20 interval improved by 2,773 m and the BI.1.20 interval by 1,981 m. This finding underscores the importance of directly incorporating the Leverett J-function method results into reservoir modeling, facilitating reservoir prediction, management, and optimizing well design and completion strategies to prevent overlooking potentially productive low-resistivity, low-contrast pays.

The application of both conventional well log interpretation and the Leverett J-function methods (which calculates water saturation independently of resistivity) for low-resistivity formations within the Lower Miocene of the Field Y is crucial for accurate reservoir characterization. Therefore, this study can be valuable in future for interpreting LRLC formations in similar fields with comparable geology and stratigraphic characteristics, ultimately contributing to improve hydrocarbon exploration and production efficiency.

## Acknowledgements

The authors would like to thank PetroVietnam and VietSovPetro for their support to publish this study. This research is funded by Vietnam National University Ho Chi Minh City (VNU-HCM) under grant number B2024-20-22. Authors thank to unknown reviewers for improving the submission.

## Literature - References

- End of Well Geological report of Well X, Field Y, Cuu Long Basin (June, 2014), Subsurface Department, MU Joint Operating Company.
- Hoang, N. V., Bach, H. V., Dung, N. T., Tam, L. T., Ha, T. V., & Trang, H. T. T. (2021). Optimal water saturation model for Miocene reservoirs in the north-eastern part of Cuu Long basin, Vietnam. *Journal of Petroleum*, 7, 16-22. <https://doi.org/10.47800/PVJ.2021.07-02>
- Phuoc, B. H. (2021). Evaluation of hydrocarbon reservoir potential in low-resistivity formations, Block 16-1, Cuu Long Basin (Doctoral dissertation). Hanoi University of Mining and Geology.
- Boyd, A., Darling, H., Tabanou, J., Davis, B., Lyon, B., Flaum, C., Klein, J., Sneider, R. M., Sibbit, A., & Singer, J. (1995). The lowdown on low resistivity pay. *Oilfield Review*, 7(3), 4-18
- Lis-Śledziona, A. (2021). Multiscale evaluation of a thin-bed reservoir. *Geology, Geophysics and Environment*, 47(1), 5-20. <https://doi.org/10.7494/geol.2021.47.1.5>

6. Shahid, M.A., Sadu, U. R, Shabbir, S. S, Muhammad, Z. H, Arshad, H. P (2008), Identification of Low Resistivity Hydrocarbon Bearing Reservoirs in Lower & Middle Indus Basin Using Available Wireline Logs, SPE Annual Technical Conference 2008
7. Yanjiao Jiang, Jian Zhou, Xiaofei Fu, Likai Cui, Chao Fang, Jiangman Cui (2021), Analyzing the Origin of Low Resistivity in Gas-Bearing Tight Sandstone Reservoir, Hindawi, Geofluids, Volume 2021, Article ID 4341804, 15 pages, <https://doi.org/10.1155/2021/4341804>
8. Fiqya Fairuz Zaemi, Rian Cahya Rohmana, Widi Atmoko (2022), Uncovering The Potential of Low Resistivity Reservoirs Through Integrated Analysis: A Case Study from The Talang Akar Formation in The South Sumatra Basin, Scientific Contributions Oil & Gas, Vol. 45. No. 3, December 2022: 169 – 181, ISSN: 2089-3361, e-ISSN: 2541-0520
9. Tolioe, W.A., M Shah B Mat Ismail, Hutajulu, A.A., Gamal Ragab Gaafar, Faizah Bt Musa, (2016) Low Resistivity Pay Evaluation, Case Study: Thin Bed Sand-Shale Lamination Reservoirs, Peninsula, Malay Basin, International Petroleum Technology Conference, IPTC-18724-MS
10. Griffiths, R., Carnegie, A., Gyllensten, A., Ribeiro, M.T. Prasodjo, A., Sallam Y., (2006) Evaluation of Low Resistivity Pay in Carbonates – A Breakthrough, SPWLA 47th Annual Logging Symposium, June 4-7, 2006
11. Shokry, I.M., Elshayeb, H., Abu-Hashish, M., (2022) Integration of conventional logs and formation micro imager for evaluation of the thinly bedded intervals in Bahariya Formation, Yomna field, Abu Al-Gharadiq Basin, Western Desert, Egypt, Journal of Applied Geophysics (Cairo) Vol. 21, Issu.1, March (2022) (pp: 1-10), ISSN: 1687-1251
12. Phuoc, B. H., Dung, P. T., Trung, L. C., & Quy, H. V. (2013). Evaluation of water saturation in the low-resistivity reservoirs of Te Giac Trang Field. Petrovietnam Journal, 7, 18-22. Retrieved from <https://pvj.com.vn/index.php/TCDK/article/view/685>
13. Tam. L. T, Hoang. C. M. Major causes of low resistivity and a model to calculate hydrocarbon saturation in the turbidite pay sands of Song Hong basin, PVN, 8/2013
14. Arifianto, I., Surjono, S.S., Erlangga, G., Abrar, B., Yogapurana, E., (2018) Application of flow zone indicator and Leverett J-function to characterise carbonate reservoir and calculate precise water saturation in the Kujung formation, North East Java Basin, Journal of Geophysics and Engineering, Volume 15, Issue 4, August 2018, Pages 1753–1766, <https://doi.org/10.1088/1742-2140/aaba2c>
15. Elgaghah, S.A., Tiab, D., and S.O. Osisanya., (2001) A New Approach for Obtaining J-Function in Clean and Shaly Reservoir Using In Situ Measurements." J Can Pet Technol 40 (2001): No Pagination Specified. DOI: <https://doi.org/10.2118/01-07-01>